

Dark matter in QCD-like theories with a theta vacuum: cosmological and astrophysical implications

Camilo García-Cely,¹ Giacomo Landini,¹ and Óscar Zapata²

¹*Instituto de Física Corpuscular (IFIC), Universitat de València-CSIC, Parc Científic UV, C/ Catedrático José Beltrán 2, E-46980 Paterna, Spain*

²*Instituto de Física, Universidad de Antioquia, Calle 70 # 52-21, Apartado Aéreo 1226, Medellín, Colombia*

QCD-like theories in which the dark matter (DM) of the Universe is hypothesized to be a thermal relic in the form of a dark pion has been extensively investigated, with most studies neglecting the CP-violating θ -angle associated with the topological vacuum. We point out that a non-vanishing θ could potentially trigger resonant number-changing processes giving rise to the observed relic density in agreement with perturbative unitarity as well as observations of clusters of galaxies. This constitutes a novel production mechanism of MeV DM and an alternative to those relying on the Wess-Zumino-Witten term. Moreover, for specific meson mass spectra, similar resonant scatterings serve as a realization of velocity-dependent self-interacting DM without a light mediator. Explicit benchmark models are presented together with a discussion of possible signals, including gravitational waves from the chiral phase transition associated with the dark pions.

Early studies of the strong-CP problem of the Standard Model (SM) [1, 2] found that the topological θ -vacuum in QCD induces cubic interactions among the pseudo-Goldstone bosons of the meson octet, which are absent for $\theta = 0$. In particular, the SM η meson may decay into two pions with a rate proportional to θ^2 . Similar interactions for pion dark matter (DM) in QCD-like theories naturally induce number-changing processes in the Early Universe (see Fig. 1), which alter the DM amount that goes out of equilibrium from the primordial plasma. We will show that this constitutes a novel production mechanism of DM in QCD-like theories. This provides an alternative to the popular SIMP model [3] of DM at the MeV scale based on $3 \rightarrow 2$ annihilations [4, 5] induced by a topological 5-point interaction, the so-called Wess-Zumino-Witten (WZW) term [6, 7]. We refer the reader to [8–32] for related work on MeV DM, and to [33–35] for studies of the effect of the θ angle in QCD-like DM models in other contexts.

Likewise, in the presence of a non-vanishing θ , resonances similar to the η meson may mediate velocity-dependent scatterings among DM pions, see Fig. 1. Such resonances have astrophysical implications [36], as velocity-dependent scatterings can diminish the central density of DM halos hosting galaxies [37, 38], while circumventing the stringent constraints on DM self-interactions derived from observations of galaxy clusters [39–43].

We will illustrate this in two specific benchmark models, one of them resembling SM QCD. We structure the discussion as follows: the first section highlights the often-overlooked interactions induced by the θ angle in QCD-like models of DM, whereas the following two sections present ensuing cosmological and astrophysical consequences. Finally, we will present a summary along with a potential outlook. In the Appendix we provide the details of our calculations.

Pion DM in a θ -vacuum. Although our conclusions apply to other gauge groups, we focus on a $SU(N_c)$

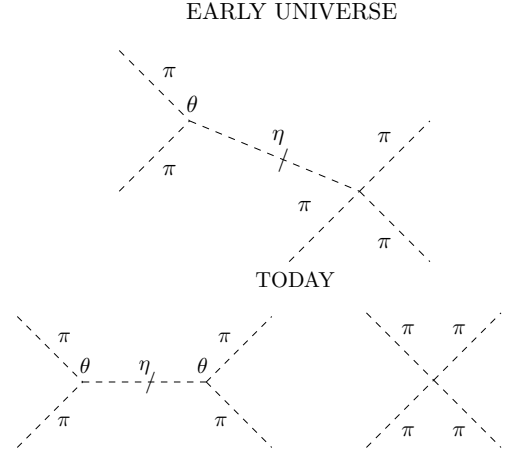


FIG. 1. The θ -vacuum could induce DM number changing processes in the early Universe and velocity-dependent self-scattering in DM halos today.

QCD-like theory of DM, with $N_c \geq 3$, and N_f flavors of light Dirac quarks in the fundamental representation. As usual, the Lagrangian reads

$$\mathcal{L} = -\frac{1}{4}F^2 + \frac{g^2\theta}{32\pi^2}F\tilde{F} + \bar{q}i\not{D}q - (\bar{q}_L M q_R + \text{h.c.}). \quad (1)$$

We assume $\theta \ll 1$ throughout for simplicity, and take $M = \text{diag}(m_1, \dots, m_{N_f})$, with $m_q \neq 0$ for all flavors. Due to the chiral anomaly, under an arbitrary transformation $q_{L,R} \rightarrow e^{\mp i\theta Q/2} q_{L,R}$, the angle in Eq. (1) shifts as $\theta \rightarrow \theta(1 - \text{Tr} Q)$ while $M \rightarrow M_\theta = e^{i\theta Q/2} M e^{i\theta Q/2}$. Taking a transformation with $\text{Tr} Q = 1$, we move the θ parameter from the $F\tilde{F}$ term to the quark mass matrix.

In analogy with ordinary QCD, we expect that strong interactions confine at some energy scale Λ , giving rise to a fermion condensate, $\langle \bar{q}q \rangle \sim \Lambda^3$. This induces a chiral phase transition (PT) for $m_q \ll \Lambda$, which spontaneously breaks the chiral flavor symmetry group of

Eq. (1): $SU(N_f)_L \times SU(N_f)_R \rightarrow SU(N_f)_V$. This leads to $N_f^2 - 1$ pseudo-Goldstone bosons, π^a , described by chiral perturbation theory (see e.g. Refs. [44, 45]), according to

$$\mathcal{L}_{\text{eff}} = \frac{f_\pi^2}{4} \text{Tr}[\partial_\mu U^\dagger \partial^\mu U] + \frac{f_\pi^2}{2} B_0 \text{Tr}[M_\theta U + U^\dagger M_\theta^\dagger], \quad (2)$$

where f_π is the dark meson constant, such that $\Lambda \sim 4\pi f_\pi / \sqrt{N_c}$, and $U = \exp(i\pi^a \lambda^a / f_\pi)$ with λ^a being the generators of $SU(N_f)$. Here the condensate is parametrized as $\langle \bar{q}q \rangle \equiv -B_0 f_\pi^2$.

The choice $Q = M^{-1} / \text{Tr} M^{-1}$ yields $\text{Tr} Q = 1$ and no linear terms in π^a in the effective Lagrangian at leading order in θ [2, 46]

$$\mathcal{L}_{\text{eff}} \supset \frac{f_\pi^2 B_0}{2} \left(\text{Tr}[M(U+U^\dagger)] + \frac{i\theta}{\text{Tr} M^{-1}} \text{Tr}[U-U^\dagger] \right). \quad (3)$$

The first term includes ordinary interactions involving an even number of mesons such as $\mathcal{L}_{\text{mass}} = -B_0 \pi^a \pi^b \text{Tr}[M\{\lambda^a, \lambda^b\}] / 4$, to be corrected by $\mathcal{O}(\theta^2)$ contributions, while the second term—often neglected—gives rise to interactions with an odd number of mesons[47]

$$\mathcal{L}_\theta = \frac{B_0 \theta}{3 f_\pi \text{Tr} M^{-1}} \left(d_{abc} \pi_a \pi_b \pi_c - \frac{c_{abcde}}{10 f_\pi^2} \pi_a \pi_b \pi_c \pi_d \pi_e \right). \quad (4)$$

Non-vanishing for $N_f \geq 3$, this allows processes absent when $\theta = 0$, particularly s -wave 3-to-2 annihilations, as pointed out in Ref. [48] for a degenerate meson spectrum. This may be compared to the topological WZW term, $\mathcal{S}_{\text{WZW}} = -i N_c \int \text{Tr}(U^\dagger dU)^5 / 240 \pi^2$, which induces a 5-point interaction [6, 7] leading to velocity suppressed 3-to-2 annihilations [3, 49].

For illustration, we consider the benchmark scenarios in table I. BM1 resembles ordinary QCD, with eight dark mesons referred to as in the SM. After accounting for the mixing angle, $\theta_{\eta\pi}$, the heaviest and lightest are respectively η and π^0 , with $m_{\pi^0} \approx m_{\pi^\pm} < m_K < m_\eta$. On the other hand, BM2 has a remnant $SU(n)$ symmetry under which the $N_f^2 - 1$ mesons organize as $n^2 - 1$ scalars in the adjoint, $2n$ scalars in the (anti)fundamental representations, K/\bar{K} , and one singlet, the η resonance. Neglecting $\mathcal{O}(\theta^2)$ corrections, the masses squared are respectively $2B_0 m$, $B_0(m + \mu)$ and $2B_0(m + n\mu) / (n + 1)$, with $\mu > m$.

Scaling as $m_\pi \sim \sqrt{m_q \Lambda}$, meson masses are naturally close to each other making plausible a spectrum with resonances. Dark baryons and dark glue-balls have typical masses of order Λ . This justifies the assumptions that the DM is made of the lightest dark meson. All mesons are stable except η , as the cubic interaction in Eq. (4) predicts

$$\Gamma(\eta \rightarrow \text{DM DM}) = \frac{\theta^2 B_0^2 \xi}{24\pi f_\pi^2 m_\eta (\text{Tr} M^{-1})^2} \sqrt{1 - \frac{4m_{\text{DM}}^2}{m_\eta^2}}, \quad (5)$$

in agreement with Refs. [1, 2, 44]. We introduce

$$v_R = 2 \sqrt{\frac{m_\eta - 2m_{\text{DM}}}{m_{\text{DM}}}}, \quad (6)$$

Benchmark	BM1	BM2
N_f	3	$n + 1$
M	$\text{diag}(m_u, m_d, m_s)$	$\text{diag}(m, \dots, m, \mu)$
Spectrum	$\pi^0, \pi^\pm, K^0, \bar{K}^0, K^\pm, \eta$	π, K, \bar{K}, η
DM particle	$\pi^0 \sim \text{singlet}$	$\pi \sim \text{adjoint of } SU(n)$
ξ in Eq. (5)	$\cos^2 3\theta_{\eta\pi}$	$6(n-1)/n$
$\langle \sigma_{\eta\pi\nu} \rangle$ in Eq. (7)	$\frac{445\sqrt{5}m_{\text{DM}}^2 \delta}{5184\pi f_\pi^4}$	$\frac{\sqrt{5}m_{\text{DM}}^2(n^2-4)}{192\pi f_\pi^4 n^2(n+1)}$
σ_0 in Eq. (8)	$\frac{m_{\text{DM}}^2}{128\pi f_\pi^4}$	$\frac{m_{\text{DM}}^2}{64\pi f_\pi^4} \frac{3n^4 - 2n^2 + 6}{n^2(n^2-1)}$

TABLE I. Benchmark models considered in this work.

to study the non-relativistic resonant effects of Fig. 1, which appear for $v_R \lesssim 1$. For BM1, up to $\mathcal{O}(v_R^2)$ and $\mathcal{O}(\theta^2)$ corrections, this fixes $\delta \equiv m_{\pi^\pm} / m_{\pi^0} - 1$ in between 0 and 0.075, depending on $r_{ud} \equiv m_u / m_d$. Further details on the mass spectrum are in the Appendix.

Cosmological implications. The θ angle impacts DM production due to the number-changing processes resulting from Eq. (4). These include 3-to-2 annihilations of DM and inverse decays $\text{DM DM} \rightarrow \eta$. As discussed below, in the absence of the resonance, the former process in our benchmarks only leads to the observed relic density in parameter space already excluded observationally. For the following discussion, we assume that the dark sector remains in kinetic equilibrium with the SM, thereby sharing the same temperature T . The model-building requirements for this are similar to those of ordinary SIMPs [3].

As in usual scenarios of co-annihilating DM, all the stable mesons eventually convert to DM with a contribution to the DM relic density that depends on their mass. Accordingly, DM and its coannihilating partners are referred to as π_{DM} . Kaons in both benchmarks are sufficiently heavy so that their contribution is exponentially suppressed and thus negligible. Consequently, $n_{\pi_{\text{DM}}} \simeq n_\pi$ in BM2. In contrast, due to $\delta \lesssim 0.075$, π^\pm in BM1 give a non-negligible contribution to the relic density, which can be calculated by noting that fast reactions $\pi^+ \pi^- \leftrightarrow \pi^0 \pi^0$ establish chemical equilibrium, $n_{\pi^0} / n_{\pi^\pm} = (n_{\pi^0} / n_{\pi^\pm})_{\text{eq}}$, allowing to write a single Boltzmann equation for the combination $n_{\pi_{\text{DM}}} = n_{\pi^0} + 2n_{\pi^\pm}$. See Ref. [26] for an extended discussion.

On the other hand, η does not behave as a co-annihilating partner but as a catalyzer [51], since it induces number-changing processes such as $\eta \pi_{\text{DM}} \rightarrow \pi_{\text{DM}} \pi_{\text{DM}}$, $\eta \rightarrow \pi_{\text{DM}} \pi_{\text{DM}}$ and their inverse. In light of this, only Boltzmann equations for η and π_{DM} are necessary.

They take a simple form in the case of most interest for this work, namely when $v_R \lesssim 0.1$ and θ is sufficiently large so that decays and inverse decays, $\eta \leftrightarrow \pi_{\text{DM}} \pi_{\text{DM}}$, are both active even after all other DM number changing interactions have frozen-out. Then, the process $\pi_{\text{DM}} \pi_{\text{DM}} \pi_{\text{DM}} \rightarrow \pi_{\text{DM}} \pi_{\text{DM}}$ is dominated by the exchange of an on-shell η resonance (see Fig. 1). In practice, this means that the 3-to-2 annihilation is a two-step process:

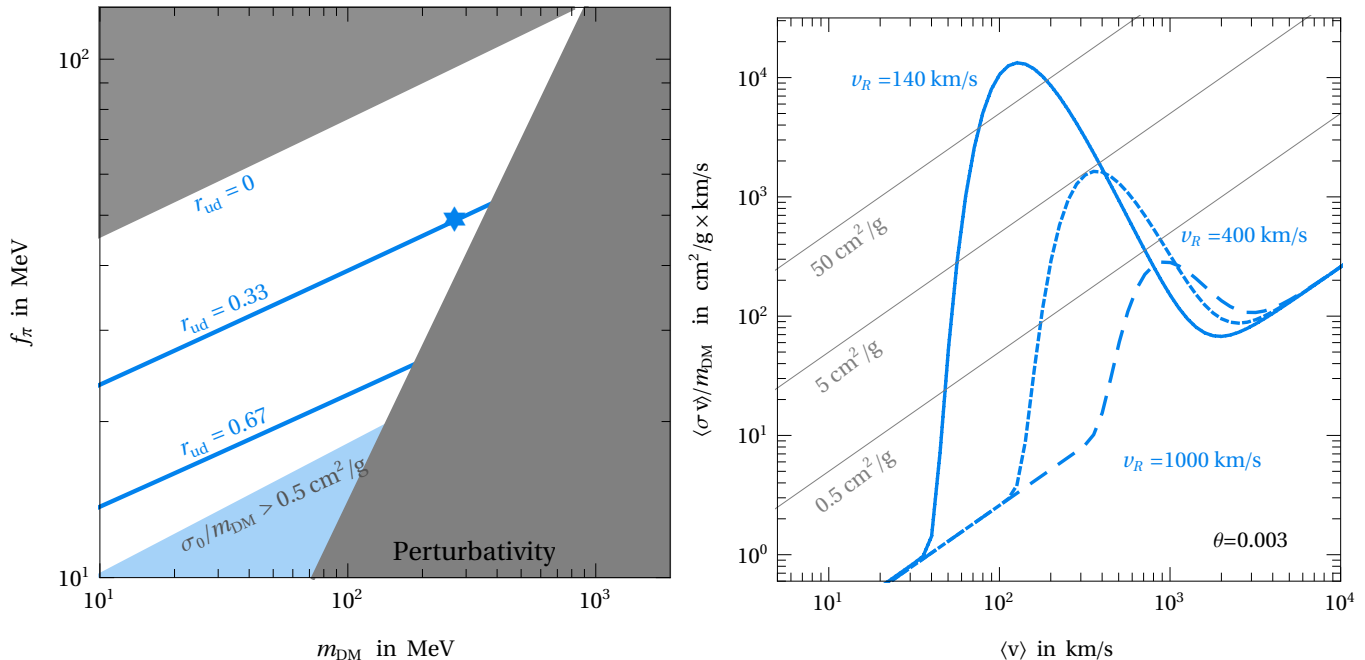


FIG. 2. *Left*: the cosmological DM relic abundance, $\Omega_{\text{DM}}h^2 = 0.12$ [50], is reproduced along the plane for different values of r_{ud} in BM1. In the upper gray region DM is overabundant for any physical value of r_{ud} , while the blue region is excluded by observations of galaxy clusters, $\sigma_0/m_{\text{DM}} > 0.5 \text{ cm}^2/\text{g}$. The star corresponds to the benchmark points plotted on the right panel. In the dark-gray region chiral perturbation theory breaks down, $m_{\text{DM}}/f_\pi > 4\pi/\sqrt{N_c}$ [49]. *Right*: Velocity dependence of the DM self-scattering cross section per unit of mass, for representative values of v_R in Eq. (6).

$\pi_{\text{DM}}\pi_{\text{DM}} \rightarrow \eta$ followed by $\eta\pi_{\text{DM}} \rightarrow \pi_{\text{DM}}\pi_{\text{DM}}$, which justifies including only these in the Boltzmann equations and neglecting the small non-resonant piece [52].

Noting that (inverse) decays do not affect $n = n_{\pi_{\text{DM}}} + 2n_\eta$, both equations combine giving $\dot{n} + 3Hn = -(n_\eta n_{\pi_{\text{DM}}} \langle \sigma_{\eta\pi} v \rangle - n_{\pi_{\text{DM}}}^2 \langle \sigma_{\pi\pi} v \rangle)$, where $\sigma_{\eta\pi} \equiv \sigma(\eta\pi_{\text{DM}} \rightarrow \pi_{\text{DM}}\pi_{\text{DM}})$, and similarly for the inverse process. This can be simplified using detailed balance, $n_\eta^{\text{eq}} \langle \sigma_{\eta\pi} v \rangle = n_{\pi_{\text{DM}}}^{\text{eq}} \langle \sigma_{\pi\pi} v \rangle$, as well as the fact that $\eta \leftrightarrow \pi_{\text{DM}}\pi_{\text{DM}}$ establish chemical equilibrium, $n_\eta/n_{\pi_{\text{DM}}}^2 = (n_\eta/n_{\pi_{\text{DM}}}^2)_{\text{eq}}$, or in terms of chemical potentials, $\mu_\eta = 2\mu_{\pi_{\text{DM}}}$. Putting everything together, the yield for the combination $Y = Y_{\pi_{\text{DM}}} + 2Y_\eta$ satisfies

$$\frac{dY}{dz} = -\langle \sigma_{\eta\pi} v \rangle \frac{s Y_{\eta,\text{eq}}}{zH} \left(\frac{Y_{\pi_{\text{DM}}}^3}{Y_{\pi_{\text{DM},\text{eq}}}^2} - \frac{Y_{\pi_{\text{DM}}}^2}{Y_{\pi_{\text{DM},\text{eq}}}} \right), \quad (7)$$

where as usual $Y_X = n_X/s$, $z \equiv m_{\text{DM}}/T$, H is the Hubble rate and s the entropy density of the Universe. The DM relic abundance is obtained upon numerical integration as $Y \simeq Y_{\pi_{\text{DM}}}$. We show our results in the left panel of Fig 2 for BM1. These are independent of v_R (if $v_R \lesssim 0.1$), but depend on δ , or equivalently on r_{ud} if the small dependence of the masses on v_R and θ is neglected. For BM2, depending on N_f , due to the large number of degenerate pions, the relic density is reproduced in parameter regions in tension with the cluster bound discussed below. This suggests that the DM must lie in a small

representation, which can be done breaking the mass degeneracy as in BM1. This is a generic feature of other color and flavor groups [53].

Notice that the relic density is independent of θ as long as $\eta \leftrightarrow \pi_{\text{DM}}\pi_{\text{DM}}$ keep the two species in chemical equilibrium at least until the time at which $\eta\pi_{\text{DM}} \rightarrow \pi_{\text{DM}}\pi_{\text{DM}}$ freezes out (see e.g. [54]). This implies a condition $\theta \geq \theta_{\text{min}}(v_R, m_{\text{DM}}, f_\pi)$, estimated requiring that the thermally-average inverse decay rate overcomes the Hubble rate at freeze-out. We find $\theta_{\text{min}} \sim 10^{-4}$ for both benchmarks. Notice also that the relic abundance is determined by s -wave 2-to-2 processes (see Table I), in contrast to the SIMP scenario based on velocity suppressed 3-to-2 annihilations.

When $\theta < \theta_{\text{min}}$ or $v_R \gg 1$, the number changing interactions in Eq. (4) lead to 3-to-2 annihilation competing with the WZW term [48]. However, in our benchmark models, these reproduce the observed DM relic density only in parameter regions excluded by cluster observations, to be discussed below.

Astrophysical implications. The θ angle could also induce resonant scattering among DM particles in present-epoch halos, see Fig. 1. The corresponding Breit-Wigner formula for the non-relativistic cross section is [36, 55]

$$\sigma(v) = \sigma_0 + \frac{128\pi}{m_{\text{DM}}^2 v_R^2 m_{\text{DM}}^2} \frac{\Gamma^2}{(v^2 - v_R^2)^2 + 4\Gamma^2 v^2/v_R^2}, \quad (8)$$

which receives a resonant enhancement for DM relative velocities, v , close to the mass combination, v_R , given in Eq. (6). For reference, in SI units, $v \sim 50$ km/s in small-scale galaxies while $v \sim 2000$ km/s in clusters of galaxies. The 1-loop η self-energy is included in $\sigma(v)$ as it impacts the scattering process [36]. The specific parameters for every benchmark are reported in Table I. We note that for BM1 all DM today consists of π^0 due to the efficient conversion of π^\pm into π^0 in the early universe [26]. Moreover, the production of π^\pm from π^0 in astrophysical halos is kinematically forbidden as $\delta \gg v^2$ today (which holds unless $\delta \lesssim 10^{-5}$, or equivalently, $r_{ud} \sim 1$). For BM2, due to the $SU(n)$ symmetry, σ_0 coincides with that reported in Ref. [3].

Clusters of galaxies constrain the self-scattering cross-section per unit mass below $0.5 \text{ cm}^2/\text{g}$ [39–43]. Regardless of v_R , the bound applies directly on σ_0/m , as depicted in Fig. 2 for each benchmark. We note that ordinary SIMPs obtaining their relic density from annihilations induced by the WZW term are in tension with this bound, as this happens in parameter regions in which $\sigma_0/m_{\text{DM}} \gtrsim 1 \text{ cm}^2/\text{g}$ (assuming chiral perturbation theory holds, i.e. $m_{\text{DM}}/f_\pi > 4\pi/\sqrt{N_c}$). The fact that the cross section is independent of the velocity when $\theta = 0$ aggravates this tension.

Eq. (8) allows for cross sections much larger than the cluster bound at small velocities. Such scatterings could serve to reconcile N-body simulations of collisionless cold DM –which predict universal halo profiles with a large central density [56–58]– with certain observations, which allegedly suggest a shallower central DM density. In fact, accounting for DM scatterings in N-body simulations indicates a reduction of the central density of such halos for $\sigma(v)/m_{\text{DM}}$ of several cm^2/g [59–64]. Known as self-interacting DM (SIDM), this is a hypothesis that has garnered attention from astronomers and particle physicists. See Refs. [38, 65] for comprehensive reviews.

In this context, Ref. [36] pointed out that the velocity dependence encoded in Eq. (8) can successfully account for the required interactions in small-scale halos while evading the constraints arising from cluster observations. Following this study, we illustrate in Fig. 2 (right panel) the velocity-average cross section at different scales for three different values of v_R . The parameters are selected such that the mechanism detailed in the preceding section yields the observed DM density. Furthermore, they are also chosen so that $\sigma(v)/m_{\text{DM}} \lesssim 100 \text{ cm}^2/\text{g}$ at $v \lesssim 100$ km/s, due to non-observation of gravothermal collapse in dwarf-sized halos [38, 65]. This is rather conservative as the observational implications of gravothermal collapse for resonant SIDM are still under investigation [66, 67] (see also Refs. [68–70]). Interestingly, the behavior in Fig. 2 is favored by observations of ultrafaint dwarf galaxies, which suggest a sharp velocity dependence [71].

Although in this letter we remain agnostic about the origin of the required values of v_R by the SIDM hypothesis –of order 10^{-4} in natural units– we highlight

that the θ angle itself could account for their smallness. For instance, any mechanism enforcing $\mu = 5m$ in BM2 leads to $v_R = 0$ for $\theta = 0$ and hence to $v_R \sim \theta$, as explained above. Furthermore, resonances with similar v_R are found in nature, for example, in resonant collisions of α -particles mediated by ${}^8\text{Be}$, a very important process in stars, where $\alpha\alpha \rightarrow {}^8\text{Be}$ followed by ${}^8\text{Be}\alpha \rightarrow {}^{12}\text{C}^*$ takes place, in analogy to the process setting the relic density above. For other examples in QCD-like models of DM, see Ref. [72].

Another signature of these scenarios is the emission of gravitational waves (GW) if the chiral PT is first order, see e.g. Refs. [73–76]. While in ordinary QCD the chiral PT is a smooth crossover [77, 78], studies of dark QCD sectors with three or more light fermions, $m_q \ll \Lambda$, establish that the PT may be first order [74], with a critical temperature $T_* \sim f_\pi$, potentially allowing for GW emission. For the specific case of $\theta = 0$, utilizing several effective models, Ref. [75] presented QCD-like benchmarks for critical temperatures of order $T_* \sim 100$ MeV with a GW spectrum peaking at frequencies in the sub-mHz band (see also Ref. [76]). On the other hand, a non-vanishing θ may affect the PT: even with the matter content of SM QCD, $\theta \sim \pi$ could render the PT first order [79], with potential consequences on the GW spectrum. This together with the fact that the dynamics of the PT and the GW spectrum depend on parameters and particle interactions not necessarily related with the pseudo-Goldstone bosons motivates a dedicated study for our benchmarks to draw conclusive statements. This is particularly important in light of the nHz signal from Pulsar Timing Arrays confirmed by the NANOGrav collaboration [80–83], which could be explained with a PT with $T_* \sim 10 - 100$ MeV [84], in precise alignment with the viable values of f_π in Fig. 2. See Ref. [85] for a hypothetical connection between the NANOGrav signal and SIDM with light mediators. The fact that our SIDM scenario does not require a light mediator could potentially alleviate the tension between this interpretation of the signal and cosmological observables requiring all unstable dark sectors particles to decay into the SM before $T \sim 1$ MeV [86].

Summary and outlook. We pointed out a production mechanism of DM in QCD-like theories where $\theta \neq 0$. This requires a resonance mediating $\pi_{\text{DM}}\pi_{\text{DM}} \rightarrow \eta$ followed by $\eta\pi_{\text{DM}} \rightarrow \pi_{\text{DM}}\pi_{\text{DM}}$, with a mass such that $v_R \lesssim 0.1$. Several resonances of this type are known to exist in the SM, particularly in the QCD sector [72]. Although it shares some similarities with theories where the relic density is obtained from annihilations induced by WZW term, here the viable parameter regions can be reconciled with cluster observations on DM self-scattering and are possibly far from the breakdown of chiral perturbation theory, see Fig. 2. This mechanism works even for small values of the topological angle, $\theta \gtrsim 10^{-4}$.

We also showed that the θ -induced scatterings might address the apparent small-scale anomalies of the collisionless cold DM paradigm. As Fig. 2 shows, self-

scattering cross sections per mass of several cm^2/g are allowed in galactic halos, simultaneously with much smaller values in galaxy clusters. Thus, the θ -vacuum leads to velocity-dependent SIDM without a light mediator, provided that $v_R \sim 100$ km/s. We emphasize that the relic density can be obtained with the mechanism mentioned above even if the SIDM hypothesis is not realized.

The θ -dependent effects discussed here are generic features of QCD-like theories. For instance, in analogy with SM, Eq. (1) exhibits an anomalous axial $U(1)$ symmetry, whose pseudo-Goldstone boson, η' , has θ -dependent cubic vertices [87, 88], potentially allowing for resonant scattering. Beyond $SU(N_c)$ gauge groups, qualitatively similar effects arise for $SO(N_c)$ or $Sp(N_c)$. In particular, with $N_c \geq 4$, gauge confinement breaks flavor symmetry as $SU(N_f) \rightarrow SO(N_f)$ for $SO(N_c)$ or $SU(N_f) \rightarrow Sp(N_f)$ for $Sp(N_c)$. This leads to Lagrangian interactions analogous to Eq. (4) if $N_f \geq 3$ for $SO(N_c)$ or $N_f \geq 6$ for $Sp(N_c)$ (see the Appendix and Refs. [89–92]). Models of this kind will be presented in an upcoming publication [53], together with an analysis of the Boltzmann equations.

Additionally, to be explored in future investigations are the CP violation effects induced by θ -angle. Following Refs. [93, 94] it would be possible to leverage the

novel source of CP violation in QCD-like sectors with a θ -angle to generate a matter-antimatter asymmetry. This approach would offer a potential workaround to the tight constraints imposed by searches for electric dipole moments in scenarios with CP-violation in the visible sector.

Acknowledgments. We thank Xiaoyong Chu, Pilar Hernández, Manoj Kaplinghat, Hyungjin Kim and Tomer Volansky for useful discussions and Ayuki Kamada for comments on the manuscript. C.G.C. is supported by a Ramón y Cajal contract with Ref. RYC2020-029248-I, the Spanish National Grant PID2022-137268NA-C55 and Generalitat Valenciana through the grant CIPROM/22/69. G.L. is supported by the Generalitat Valenciana APOSTD/2023 Grant No. CIAPOS/2022/193. G.L. also acknowledges the hospitality of Universidade de Coimbra, Portugal. O.Z. has been partially supported by Sostenibilidad-UdeA, the UdeA/CODI Grants 2022-52380 and 2023-59130, and Ministerio de Ciencias Grant CD 82315 CT ICETEX 2021-1080. O.Z. also acknowledges the support of the Simons Foundation under Award number 1023171-RC and the hospitality of the International Institute of Physics at the Universidade Federal do Rio Grande do Norte in Natal, Brazil.

-
- [1] M. A. Shifman, A. I. Vainshtein, and V. I. Zakharov, “Can Confinement Ensure Natural CP Invariance of Strong Interactions?,” *Nucl. Phys. B* **166** (1980) 493–506.
- [2] R. J. Crewther, P. Di Vecchia, G. Veneziano, and E. Witten, “Chiral Estimate of the Electric Dipole Moment of the Neutron in Quantum Chromodynamics,” *Phys. Lett. B* **88** (1979) 123. [Erratum: *Phys.Lett.B* 91, 487 (1980)].
- [3] Y. Hochberg, E. Kuflik, H. Murayama, T. Volansky, and J. G. Wacker, “Model for Thermal Relic Dark Matter of Strongly Interacting Massive Particles,” *Phys. Rev. Lett.* **115** no. 2, (2015) 021301, [arXiv:1411.3727 \[hep-ph\]](#).
- [4] E. D. Carlson, M. E. Machacek, and L. J. Hall, “Self-interacting dark matter,” *Astrophys. J.* **398** (1992) 43–52.
- [5] Y. Hochberg, E. Kuflik, T. Volansky, and J. G. Wacker, “Mechanism for Thermal Relic Dark Matter of Strongly Interacting Massive Particles,” *Phys. Rev. Lett.* **113** (2014) 171301, [arXiv:1402.5143 \[hep-ph\]](#).
- [6] J. Wess and B. Zumino, “Consequences of anomalous Ward identities,” *Phys. Lett. B* **37** (1971) 95–97.
- [7] E. Witten, “Global Aspects of Current Algebra,” *Nucl. Phys. B* **223** (1983) 422–432.
- [8] Y. Hochberg, E. Kuflik, and H. Murayama, “SIMP Spectroscopy,” *JHEP* **05** (2016) 090, [arXiv:1512.07917 \[hep-ph\]](#).
- [9] E. Kuflik, M. Perelstein, N. R.-L. Lorier, and Y.-D. Tsai, “Elastically Decoupling Dark Matter,” *Phys. Rev. Lett.* **116** no. 22, (2016) 221302, [arXiv:1512.04545 \[hep-ph\]](#).
- [10] N. Bernal, C. Garcia-Cely, and R. Rosenfeld, “WIMP and SIMP Dark Matter from the Spontaneous Breaking of a Global Group,” *JCAP* **04** (2015) 012, [arXiv:1501.01973 \[hep-ph\]](#).
- [11] N. Bernal and X. Chu, “ \mathbb{Z}_2 SIMP Dark Matter,” *JCAP* **01** (2016) 006, [arXiv:1510.08527 \[hep-ph\]](#).
- [12] N. Bernal, X. Chu, C. Garcia-Cely, T. Hambye, and B. Zaldivar, “Production Regimes for Self-Interacting Dark Matter,” *JCAP* **03** (2016) 018, [arXiv:1510.08063 \[hep-ph\]](#).
- [13] S.-M. Choi and H. M. Lee, “SIMP dark matter with gauged Z_3 symmetry,” *JHEP* **09** (2015) 063, [arXiv:1505.00960 \[hep-ph\]](#).
- [14] S.-M. Choi and H. M. Lee, “Resonant SIMP dark matter,” *Phys. Lett. B* **758** (2016) 47–53, [arXiv:1601.03566 \[hep-ph\]](#).
- [15] A. Soni and Y. Zhang, “Hidden $SU(N)$ Glueball Dark Matter,” *Phys. Rev. D* **93** no. 11, (2016) 115025, [arXiv:1602.00714 \[hep-ph\]](#).
- [16] A. Kamada, M. Yamada, T. T. Yanagida, and K. Yonekura, “SIMP from a strong $U(1)$ gauge theory with a monopole condensation,” *Phys. Rev. D* **94** no. 5, (2016) 055035, [arXiv:1606.01628 \[hep-ph\]](#).
- [17] N. Bernal, X. Chu, and J. Pradler, “Simply split strongly interacting massive particles,” *Phys. Rev. D* **95** no. 11, (2017) 115023, [arXiv:1702.04906 \[hep-ph\]](#).
- [18] J. M. Cline, H. Liu, T. Slatyer, and W. Xue, “Enabling Forbidden Dark Matter,” *Phys. Rev. D* **96** no. 8, (2017) 083521, [arXiv:1702.07716 \[hep-ph\]](#).
- [19] S.-M. Choi, H. M. Lee, and M.-S. Seo, “Cosmic abundances of SIMP dark matter,” *JHEP* **04** (2017) 154, [arXiv:1702.07860 \[hep-ph\]](#).
- [20] E. Kuflik, M. Perelstein, N. R.-L. Lorier, and Y.-D.

- Tsai, “Phenomenology of ELDER Dark Matter,” *JHEP* **08** (2017) 078, [arXiv:1706.05381 \[hep-ph\]](#).
- [21] M. Heikinheimo, K. Tuominen, and K. Langæble, “Hidden strongly interacting massive particles,” *Phys. Rev. D* **97** no. 9, (2018) 095040, [arXiv:1803.07518 \[hep-ph\]](#).
- [22] S.-M. Choi, H. M. Lee, P. Ko, and A. Natale, “Resolving phenomenological problems with strongly-interacting-massive-particle models with dark vector resonances,” *Phys. Rev. D* **98** no. 1, (2018) 015034, [arXiv:1801.07726 \[hep-ph\]](#).
- [23] Y. Hochberg, E. Kuflik, R. McGehee, H. Murayama, and K. Schutz, “Strongly interacting massive particles through the axion portal,” *Phys. Rev. D* **98** no. 11, (2018) 115031, [arXiv:1806.10139 \[hep-ph\]](#).
- [24] N. Bernal, X. Chu, S. Kulkarni, and J. Pradler, “Self-interacting dark matter without prejudice,” *Phys. Rev. D* **101** no. 5, (2020) 055044, [arXiv:1912.06681 \[hep-ph\]](#).
- [25] S.-M. Choi, H. M. Lee, Y. Mambri, and M. Pierre, “Vector SIMP dark matter with approximate custodial symmetry,” *JHEP* **07** (2019) 049, [arXiv:1904.04109 \[hep-ph\]](#).
- [26] A. Katz, E. Salvioni, and B. Shakya, “Split SIMPs with Decays,” *JHEP* **10** (2020) 049, [arXiv:2006.15148 \[hep-ph\]](#).
- [27] J. Smirnov and J. F. Beacom, “New Freezeout Mechanism for Strongly Interacting Dark Matter,” *Phys. Rev. Lett.* **125** no. 13, (2020) 131301, [arXiv:2002.04038 \[hep-ph\]](#).
- [28] C.-Y. Xing and S.-H. Zhu, “Dark Matter Freeze-Out via Catalyzed Annihilation,” *Phys. Rev. Lett.* **127** no. 6, (2021) 061101, [arXiv:2102.02447 \[hep-ph\]](#).
- [29] P. Braat and M. Postma, “SIMPLY add a dark photon,” *JHEP* **03** (2023) 216, [arXiv:2301.04513 \[hep-ph\]](#).
- [30] E. Bernreuther, N. Hemme, F. Kahlhoefer, and S. Kulkarni, “Dark matter relic density in strongly interacting dark sectors with light vector mesons,” [arXiv:2311.17157 \[hep-ph\]](#).
- [31] R. Garani, M. Redi, and A. Tesi, “Dark QCD matters,” *JHEP* **12** (2021) 139, [arXiv:2105.03429 \[hep-ph\]](#).
- [32] U. K. Dey, T. N. Maity, and T. S. Ray, “Light Dark Matter through Assisted Annihilation,” *JCAP* **03** (2017) 045, [arXiv:1612.09074 \[hep-ph\]](#).
- [33] M. Redi, A. Strumia, A. Tesi, and E. Vigiani, “Di-photon resonance and Dark Matter as heavy pions,” *JHEP* **05** (2016) 078, [arXiv:1602.07297 \[hep-ph\]](#).
- [34] P. Draper, J. Kozaczuk, and J.-H. Yu, “Theta in new QCD-like sectors,” *Phys. Rev. D* **98** no. 1, (2018) 015028, [arXiv:1803.00015 \[hep-ph\]](#).
- [35] T. Abe, R. Sato, and T. Yamanaka, “Composite Dark Matter with Forbidden Annihilation,” [arXiv:2404.03963 \[hep-ph\]](#).
- [36] X. Chu, C. Garcia-Cely, and H. Murayama, “Velocity Dependence on Resonant Self-Interacting Dark Matter,” *Phys. Rev. Lett.* **122** no. 7, (2019) 071103, [arXiv:1810.04709 \[hep-ph\]](#).
- [37] D. N. Spergel and P. J. Steinhardt, “Observational evidence for selfinteracting cold dark matter,” *Phys. Rev. Lett.* **84** (2000) 3760–3763, [arXiv:astro-ph/9909386](#).
- [38] S. Tulin and H.-B. Yu, “Dark Matter Self-interactions and Small Scale Structure,” *Phys. Rept.* **730** (2018) 1–57, [arXiv:1705.02358 \[hep-ph\]](#).
- [39] D. Harvey, R. Massey, T. Kitching, A. Taylor, and E. Tittley, “The non-gravitational interactions of dark matter in colliding galaxy clusters,” *Science* **347** (2015) 1462–1465, [arXiv:1503.07675 \[astro-ph.CO\]](#).
- [40] K. Bondarenko, A. Boyarsky, T. Bringmann, and A. Sokolenko, “Constraining self-interacting dark matter with scaling laws of observed halo surface densities,” *JCAP* **04** (2018) 049, [arXiv:1712.06602 \[astro-ph.CO\]](#).
- [41] D. Harvey, A. Robertson, R. Massey, and I. G. McCarthy, “Observable tests of self-interacting dark matter in galaxy clusters: BCG wobbles in a constant density core,” *Mon. Not. Roy. Astron. Soc.* **488** no. 2, (2019) 1572–1579, [arXiv:1812.06981 \[astro-ph.CO\]](#).
- [42] L. Sagunski, S. Gad-Nasr, B. Colquhoun, A. Robertson, and S. Tulin, “Velocity-dependent Self-interacting Dark Matter from Groups and Clusters of Galaxies,” *JCAP* **01** (2021) 024, [arXiv:2006.12515 \[astro-ph.CO\]](#).
- [43] **DES Collaboration**, D. Cross et al., “Examining the self-interaction of dark matter through central cluster galaxy offsets,” *Mon. Not. Roy. Astron. Soc.* **529** no. 1, (2024) 52–58, [arXiv:2304.10128 \[astro-ph.CO\]](#).
- [44] A. Pich and E. de Rafael, “Strong CP violation in an effective chiral Lagrangian approach,” *Nucl. Phys. B* **367** (1991) 313–333.
- [45] S. Scherer, “Introduction to chiral perturbation theory,” *Adv. Nucl. Phys.* **27** (2003) 277, [arXiv:hep-ph/0210398](#).
- [46] L. Di Luzio, M. Giannotti, E. Nardi, and L. Visinelli, “The landscape of QCD axion models,” *Phys. Rept.* **870** (2020) 1–117, [arXiv:2003.01100 \[hep-ph\]](#).
- [47] Throughout $\text{Tr}[\lambda_a \lambda_b] = 2\delta_{ab}$, while the symmetric tensors are $d_{abc} = \frac{1}{4}\text{Tr}(\{\lambda_a, \lambda_b\}\lambda_c)$, and $c_{abcde} = (\delta_{abd}c_{cde} + \delta_{cd}d_{abe})/N_f + \frac{1}{2}d_{abm}d_{cdn}d_{mne}$.
- [48] A. Kamada, H. Kim, and T. Sekiguchi, “Axionlike particle assisted strongly interacting massive particle,” *Phys. Rev. D* **96** no. 1, (2017) 016007, [arXiv:1704.04505 \[hep-ph\]](#).
- [49] A. Kamada, S. Kobayashi, and T. Kuwahara, “Perturbative unitarity of strongly interacting massive particle models,” *JHEP* **02** (2023) 217, [arXiv:2210.01393 \[hep-ph\]](#).
- [50] **Planck Collaboration**, N. Aghanim et al., “Planck 2018 results. VI. Cosmological parameters,” *Astron. Astrophys.* **641** (2020) A6, [arXiv:1807.06209 \[astro-ph.CO\]](#). [Erratum: *Astron. Astrophys.* 652, C4 (2021)].
- [51] X. Chu, M. Nikolic, and J. Pradler, “Even SIMP miracles are possible,” [arXiv:2401.12283 \[hep-ph\]](#).
- [52] E. W. Kolb and S. Wolfram, “Baryon Number Generation in the Early Universe,” *Nucl. Phys. B* **172** (1980) 224. [Erratum: *Nucl. Phys. B* 195, 542 (1982)].
- [53] C. García-Cely, G. Landini, L. Marsili, and O. Zapata *In preparation* (2024).
- [54] R. Frumkin, Y. Hochberg, E. Kuflik, and H. Murayama, “Thermal Dark Matter from Freeze-Out of Inverse Decays,” *Phys. Rev. Lett.* **130** no. 12, (2023) 121001, [arXiv:2111.14857 \[hep-ph\]](#).
- [55] X. Chu, C. Garcia-Cely, and H. Murayama, “A Practical and Consistent Parametrization of Dark Matter Self-Interactions,” *JCAP* **06** (2020) 043, [arXiv:1908.06067 \[hep-ph\]](#).
- [56] J. Dubinski and R. G. Carlberg, “The Structure of cold

- dark matter halos,” *Astrophys. J.* **378** (1991) 496.
- [57] J. F. Navarro, C. S. Frenk, and S. D. M. White, “The Structure of cold dark matter halos,” *Astrophys. J.* **462** (1996) 563–575, [arXiv:astro-ph/9508025](#).
- [58] J. F. Navarro, C. S. Frenk, and S. D. M. White, “A Universal density profile from hierarchical clustering,” *Astrophys. J.* **490** (1997) 493–508, [arXiv:astro-ph/9611107](#).
- [59] R. Dave, D. N. Spergel, P. J. Steinhardt, and B. D. Wandelt, “Halo properties in cosmological simulations of selfinteracting cold dark matter,” *Astrophys. J.* **547** (2001) 574–589, [arXiv:astro-ph/0006218](#).
- [60] M. Vogelsberger, J. Zavala, and A. Loeb, “Subhaloes in Self-Interacting Galactic Dark Matter Haloes,” *Mon. Not. Roy. Astron. Soc.* **423** (2012) 3740, [arXiv:1201.5892 \[astro-ph.CO\]](#).
- [61] M. Rocha, A. H. G. Peter, J. S. Bullock, M. Kaplinghat, S. Garrison-Kimmel, J. Onorbe, and L. A. Moustakas, “Cosmological Simulations with Self-Interacting Dark Matter I: Constant Density Cores and Substructure,” *Mon. Not. Roy. Astron. Soc.* **430** (2013) 81–104, [arXiv:1208.3025 \[astro-ph.CO\]](#).
- [62] A. H. G. Peter, M. Rocha, J. S. Bullock, and M. Kaplinghat, “Cosmological Simulations with Self-Interacting Dark Matter II: Halo Shapes vs. Observations,” *Mon. Not. Roy. Astron. Soc.* **430** (2013) 105, [arXiv:1208.3026 \[astro-ph.CO\]](#).
- [63] O. D. Elbert, J. S. Bullock, S. Garrison-Kimmel, M. Rocha, J. Onorbe, and A. H. G. Peter, “Core formation in dwarf haloes with self-interacting dark matter: no fine-tuning necessary,” *Mon. Not. Roy. Astron. Soc.* **453** no. 1, (2015) 29–37, [arXiv:1412.1477 \[astro-ph.GA\]](#).
- [64] A. B. Fry, F. Governato, A. Pontzen, T. Quinn, M. Tremmel, L. Anderson, H. Menon, A. M. Brooks, and J. Wadsley, “All about baryons: revisiting SIDM predictions at small halo masses,” *Mon. Not. Roy. Astron. Soc.* **452** no. 2, (2015) 1468–1479, [arXiv:1501.00497 \[astro-ph.CO\]](#).
- [65] S. Adhikari et al., “Astrophysical Tests of Dark Matter Self-Interactions,” [arXiv:2207.10638 \[astro-ph.CO\]](#).
- [66] V. Tran, D. Gilman, M. Vogelsberger, X. Shen, S. O’Neil, and X. Zhang, “Gravothermal Catastrophe in Resonant Self-interacting Dark Matter Models,” [arXiv:2405.02388 \[astro-ph.GA\]](#).
- [67] A. Kamada and H. J. Kim, “Evolution of resonant self-interacting dark matter halos,” *Phys. Rev. D* **109** no. 6, (2024) 063535, [arXiv:2304.12621 \[astro-ph.CO\]](#).
- [68] D. Yang and H.-B. Yu, “Gravothermal evolution of dark matter halos with differential elastic scattering,” *JCAP* **09** (2022) 077, [arXiv:2205.03392 \[astro-ph.CO\]](#).
- [69] S. Yang, X. Du, Z. C. Zeng, A. Benson, F. Jiang, E. O. Nadler, and A. H. G. Peter, “Gravothermal Solutions of SIDM Halos: Mapping from Constant to Velocity-dependent Cross Section,” *Astrophys. J.* **946** no. 1, (2023) 47, [arXiv:2205.02957 \[astro-ph.CO\]](#).
- [70] N. J. Outmezguine, K. K. Boddy, S. Gad-Nasr, M. Kaplinghat, and L. Sagunski, “Universal gravothermal evolution of isolated self-interacting dark matter halos for velocity-dependent cross-sections,” *Mon. Not. Roy. Astron. Soc.* **523** no. 3, (2023) 4786–4800, [arXiv:2204.06568 \[astro-ph.GA\]](#).
- [71] K. Hayashi, M. Ibe, S. Kobayashi, Y. Nakayama, and S. Shirai, “Probing dark matter self-interaction with ultrafaint dwarf galaxies,” *Phys. Rev. D* **103** no. 2, (2021) 023017, [arXiv:2008.02529 \[astro-ph.CO\]](#).
- [72] Y.-D. Tsai, R. McGehee, and H. Murayama, “Resonant Self-Interacting Dark Matter from Dark QCD,” *Phys. Rev. Lett.* **128** no. 17, (2022) 172001, [arXiv:2008.08608 \[hep-ph\]](#).
- [73] E. Witten, “Cosmic Separation of Phases,” *Phys. Rev. D* **30** (1984) 272–285.
- [74] P. Schwaller, “Gravitational Waves from a Dark Phase Transition,” *Phys. Rev. Lett.* **115** no. 18, (2015) 181101, [arXiv:1504.07263 \[hep-ph\]](#).
- [75] A. J. Helmboldt, J. Kubo, and S. van der Woude, “Observational prospects for gravitational waves from hidden or dark chiral phase transitions,” *Phys. Rev. D* **100** no. 5, (2019) 055025, [arXiv:1904.07891 \[hep-ph\]](#).
- [76] M. Reichert, F. Sannino, Z.-W. Wang, and C. Zhang, “Dark confinement and chiral phase transitions: gravitational waves vs matter representations,” *JHEP* **01** (2022) 003, [arXiv:2109.11552 \[hep-ph\]](#).
- [77] Y. Aoki, G. Endrodi, Z. Fodor, S. D. Katz, and K. K. Szabo, “The Order of the quantum chromodynamics transition predicted by the standard model of particle physics,” *Nature* **443** (2006) 675–678, [arXiv:hep-lat/0611014](#).
- [78] T. Bhattacharya et al., “QCD Phase Transition with Chiral Quarks and Physical Quark Masses,” *Phys. Rev. Lett.* **113** no. 8, (2014) 082001, [arXiv:1402.5175 \[hep-lat\]](#).
- [79] Y. Bai, T.-K. Chen, and M. Korwar, “QCD-collapsed domain walls: QCD phase transition and gravitational wave spectroscopy,” *JHEP* **12** (2023) 194, [arXiv:2306.17160 \[hep-ph\]](#).
- [80] **EPTA, InPTA: Collaboration**, J. Antoniadis et al., “The second data release from the European Pulsar Timing Array - III. Search for gravitational wave signals,” *Astron. Astrophys.* **678** (2023) A50, [arXiv:2306.16214 \[astro-ph.HE\]](#).
- [81] D. J. Reardon et al., “Search for an Isotropic Gravitational-wave Background with the Parkes Pulsar Timing Array,” *Astrophys. J. Lett.* **951** no. 1, (2023) L6, [arXiv:2306.16215 \[astro-ph.HE\]](#).
- [82] **NANOGrav Collaboration**, G. Agazie et al., “The NANOGrav 15 yr Data Set: Evidence for a Gravitational-wave Background,” *Astrophys. J. Lett.* **951** no. 1, (2023) L8, [arXiv:2306.16213 \[astro-ph.HE\]](#).
- [83] H. Xu et al., “Searching for the Nano-Hertz Stochastic Gravitational Wave Background with the Chinese Pulsar Timing Array Data Release I,” *Res. Astron. Astrophys.* **23** no. 7, (2023) 075024, [arXiv:2306.16216 \[astro-ph.HE\]](#).
- [84] **NANOGrav Collaboration**, A. Afzal et al., “The NANOGrav 15 yr Data Set: Search for Signals from New Physics,” *Astrophys. J. Lett.* **951** no. 1, (2023) L11, [arXiv:2306.16219 \[astro-ph.HE\]](#).
- [85] C. Han, K.-P. Xie, J. M. Yang, and M. Zhang, “Self-interacting dark matter implied by nano-Hertz gravitational waves,” [arXiv:2306.16966 \[hep-ph\]](#).
- [86] T. Bringmann, P. F. Depta, T. Konstandin, K. Schmidt-Hoberg, and C. Tasillo, “Does NANOGrav observe a dark sector phase transition?,” *JCAP* **11** (2023) 053, [arXiv:2306.09411 \[astro-ph.CO\]](#).
- [87] E. Witten, “Large N Chiral Dynamics,” *Annals Phys.*

- [128](#) (1980) 363.
- [88] P. Di Vecchia and G. Veneziano, “Chiral Dynamics in the Large n Limit,” *Nucl. Phys. B* **171** (1980) 253–272.
- [89] F. Sannino, A. Strumia, A. Tesi, and E. Vigiani, “Fundamental partial compositeness,” *JHEP* **11** (2016) 029, [arXiv:1607.01659 \[hep-ph\]](#).
- [90] G. Landini, *Dark Matter and gauge dynamics*. PhD thesis, Pisa University, 2022.
- [91] D. Buttazzo, L. Di Luzio, P. Ghorbani, C. Gross, G. Landini, A. Strumia, D. Teresi, and J.-W. Wang, “Scalar gauge dynamics and Dark Matter,” *JHEP* **01** (2020) 130, [arXiv:1911.04502 \[hep-ph\]](#).
- [92] E. Witten, “An $SU(2)$ Anomaly,” *Phys. Lett. B* **117** (1982) 324–328.
- [93] J. M. Cline, K. Kainulainen, and D. Tucker-Smith, “Electroweak baryogenesis from a dark sector,” *Phys. Rev. D* **95** no. 11, (2017) 115006, [arXiv:1702.08909 \[hep-ph\]](#).
- [94] M. Carena, M. Quirós, and Y. Zhang, “Electroweak Baryogenesis from Dark-Sector CP Violation,” *Phys. Rev. Lett.* **122** no. 20, (2019) 201802, [arXiv:1811.09719 \[hep-ph\]](#).

Appendix A: Chiral Lagrangians in a θ -vacuum

In the main text we illustrate the effects of a non-vanishing θ angle in a dark $SU(N_c)$ QCD-like theory with N_f flavors of light fermions in the fundamental representation and $N_c \geq 3$. Our results can be easily generalized to other choices of the gauge group, namely $SO(N_c)$ or $Sp(N_c)$. We first summarize the $SU(N_c)$ case and then discuss the other possibilities.

Unitary groups. The Lagrangian describing N_f massless Dirac fermions in the fundamental representation of a $SU(N_c)$ gauge group with $N_c \geq 3$ enjoys a global flavor symmetry, $G_F = SU(N_f)_L \times SU(N_f)_R$, under which the fermion chiral components transform as $q_{L(R)} \rightarrow \exp(i\alpha_{L(R)}^a \lambda^a) q_{L(R)}$, where λ^a are the generators of $SU(N_f)$ normalized as $\text{Tr}(\lambda^a \lambda^b) = 2\delta^{ab}$. Confinement of gauge interactions induces a fermion condensate $\langle \bar{q}q \rangle \sim \Lambda^3$ which spontaneously breaks the flavor group $SU(N_f)_L \otimes SU(N_f)_R \rightarrow SU(N_f)_V$. The unbroken vectorial subgroup is defined as the set of transformations for which $\alpha_L^a = \alpha_R^a$. This gives rise to $N_f^2 - 1$ Goldstone bosons, π^a , living in the coset space $(SU(N_f)_L \otimes SU(N_f)_R)/SU(N_f)_V \sim SU(N_f)$. Their interactions are described by the effective Lagrangian $\mathcal{L}_{\text{eff}}^{M=0} = f_\pi^2 \text{Tr}[\partial_\mu U^\dagger \partial^\mu U]/4$, where $U = e^{i\Pi/f_\pi}$, with $\Pi = \pi^a \lambda^a$. A quark mass matrix M explicitly breaks the flavor symmetry group G_F . However, if $m_q \ll \Lambda$, G_F is still a good approximate symmetry, in which case, the small breaking due to the mass matrix is parametrized in the effective Lagrangian as

$$\mathcal{L}_{\text{eff}} = \frac{f_\pi^2}{4} \text{Tr}[\partial_\mu U^\dagger \partial^\mu U] + \frac{f_\pi^2}{2} B_0 \text{Tr}[M_\theta U + U^\dagger M_\theta^\dagger]. \quad (\text{A1})$$

Here, we include the effect of a non-vanishing θ term as $M_\theta = e^{i\theta Q/2} M e^{i\theta Q/2}$, with $Q = M^{-1}/\text{Tr}M^{-1}$. The π^a acquire a small mass $m_\pi \sim \sqrt{m_q \Lambda} \ll \Lambda$, becoming pseudo-Goldstone bosons.

The presence of $\theta \neq 0$ generates interactions involving an odd number of mesons. The leading terms are

$$\mathcal{L}_\theta = \frac{\theta}{6f_\pi \text{Tr}M^{-1}} B_0 \text{Tr}\Pi^3 - \frac{\theta}{120f_\pi^3 \text{Tr}M^{-1}} B_0 \text{Tr}\Pi^5, \quad (\text{A2})$$

which gives rise to decays $\pi^a \rightarrow \pi^b \pi^c$, as well as 3-to-2 processes $\pi^a \pi^b \pi^c \rightarrow \pi^d \pi^e$. We introduce the $SU(N)$ structure constants: the totally anti-symmetric $f_{abc} = -i\text{Tr}([\lambda_a, \lambda_b] \lambda_c)/4$ and the totally symmetric $d_{abc} = \text{Tr}(\{\lambda_a, \lambda_b\} \lambda_c)/4$. Using the $SU(N)$ identity $\text{Tr}(\lambda_a \lambda_b \lambda_c) = 2(d_{abc} + if_{abc})$ and the symmetry properties of the structure constants we get

$$\mathcal{L}_\theta = \frac{B_0 \theta}{3f_\pi \text{Tr}M^{-1}} \left(d_{abc} \pi_a \pi_b \pi_c - \frac{c_{abcde}}{10f_\pi^2} \pi_a \pi_b \pi_c \pi_d \pi_e \right), \quad (\text{A3})$$

where $c_{abcde} = (\delta_{ab} d_{cde} + \delta_{cd} d_{abe})/N_f + \frac{1}{2} d_{abm} d_{cdn} d_{mne}$. These interactions are present whenever the d_{abc} tensor is non-vanishing, which occurs if $N_f \geq 3$.

Finally, the Lagrangian must be augmented with the well-known Wess-Zumino-Witten (WZW) term, describing the 5-point interaction

$$\mathcal{L}_{\text{WZW}} = -\frac{N_c}{240\pi^2 f_\pi^5} \epsilon^{\mu\nu\rho\sigma} \text{Tr}[\Pi \partial_\mu \Pi \partial_\nu \Pi \partial_\rho \Pi \partial_\sigma \Pi]. \quad (\text{A4})$$

The WZW term induces an extra contribution to 3-to-2 processes $\pi^a \pi^b \pi^c \rightarrow \pi^d \pi^e$, which competes with that of θ and is non-vanishing if the coset space has a non-trivial fifth homotopy group, π_5 . For unitary gauge groups, this occurs when $N_f \geq 3$, as in such a case $\pi_5(SU(N_f)) = \mathbb{Z}$.

The case $N_c = 2$ is special as the flavor group is $SU(2N_f)$, whose corresponding fermion condensate breaks to $Sp(2N_f)$, giving rise to $2N_f^2 - N_f - 1$ pseudo-Goldstone bosons. Similar to the case of $Sp(N_c)$ discussed below, for $N_f \geq 3$ the d_{abc} tensors do not vanish, while WZW term appears already for $N_f \geq 2$.

Orthogonal groups. The Lagrangian of N_f massless Weyl fermions in the fundamental representation of $SO(N_c)$ enjoys a $SU(N_f)$ flavor symmetry. As usual, we consider $N_c \geq 4$ because $N_c = 2$ and $N_c = 3$ respectively correspond to $U(1)$ and $SU(2)$. The fermion condensate $\langle qq \rangle$ spontaneously breaks the flavor symmetry as $SU(N_f) \rightarrow SO(N_f)$, leading to $N_f(N_f+1)/2 - 1$ pseudo-Goldstone bosons. Their dynamics is described again by Eq. (A1) with the λ^a matrices in the U field replaced with the elements of the coset $SU(N_f)/SO(N_f)$, which are the real generators of $SU(N_f)$. Note that the real generators of $SU(N_f)$ are symmetric while the imaginary ones are antisymmetric and correspond to those of $SO(N_f)$. The odd interactions in Eq. (A3) are present if the symmetric d_{abc} tensor is non-vanishing, which occurs if $N_f \geq 3$. The WZW term is non-vanishing also for $N_f \geq 3$ as in that case $\pi_5(SU(N_f)/SO(N_f)) = \mathbb{Z}$ [3, 89].

Symplectic groups. The Lagrangian of N_f massless Weyl fermions in the fundamental representation of a $Sp(N_c)$ gauge group enjoys a $SU(N_f)$ flavor symmetry, which is broken as $SU(N_f) \rightarrow Sp(N_f)$ by the fermion

condensate. Notice that N_c needs to be an even integer for symplectic groups, and without loss of generality, $N_c \geq 4$ as $Sp(2) = SU(2)$. Furthermore, N_f must be even to avoid the global anomaly of the gauge group [92]. The number of pseudo-Goldstone bosons is $N_f(N_f - 1)/2 - 1$. The interactions among the mesons are described again by Eq. (A1) with the meson field replaced by $U = e^{i\pi^a \lambda^a / f_\pi} \gamma_{N_f}$, where $\gamma_{N_f} \equiv \mathbf{1}_{N_f/2} \otimes i\sigma_2$ is the antisymmetric invariant tensor of $Sp(N_f)$. Here, the λ^a matrices are the elements of the coset $SU(N_f)/Sp(N_f)$ which can be expressed as $\{\tilde{\lambda}_R^a \otimes \mathbf{1}_2, \tilde{\lambda}_I^a \otimes \sigma_k\}/\sqrt{2}$, where $\tilde{\lambda}_{R(I)}^a$ are the real symmetric (imaginary anti-symmetric) generators of $SU(N_f/2)$ and σ_k are the Pauli matrices, see e.g. Refs. [90, 91]. The d_{abc} tensor entering the odd interactions is non-vanishing for $N_f \geq 6$, see e.g. Ref. [48], while the WZW term is non-vanishing for $N_f \geq 4$ as $\pi_5(SU(N_f)/Sp(N_f)) = \mathbb{Z}$ in that case [3].

Appendix B: Explicit Lagrangian for each benchmark

Tadpoles. The interactions described in the chiral Lagrangian of Eq. (A1) induce tadpoles, i.e. linear terms in the meson field $\Pi = \pi^a \lambda^a$. At leading order in θ , these arise in the form $\text{Tr}[\Pi\{M, Q\}]$. Choosing $Q = M^{-1}/\text{Tr}M^{-1}$, which satisfies $\text{Tr}Q = 1$, and using $\text{Tr}\Pi = 0$, the linear terms vanish and Lagrangian takes the form of Eq. (3) of the main text up to $\mathcal{O}(\theta^2)$ corrections. At higher orders in θ , one must choose a more involved function $Q(\theta)$, which reduces to the expression above for $\theta \ll 1$.

Mass spectrum. The mass spectrum of the mesons is obtained expanding at the quadratic order in Π , which gives $\mathcal{L}_{\text{mass}} = -B_0 \pi^a \pi^b \text{Tr}[M\{\lambda^a, \lambda^b\}]/4 + \mathcal{O}(\theta^2)$. In the following we present the details for the two benchmark models discussed in the main text.

- *Benchmark BM1.* We fix $N_f = 3$ and we adopt the same notation of ordinary QCD. The quark mass matrix is $M = \text{diag}(m_u, m_d, m_s)$ with $m_u \leq m_d \leq m_s$. The spectrum consists of 8 pseudo-Goldstone bosons: $\pi^\pm = (\pi_1 \pm i\pi_2)/\sqrt{2}$, $K^\pm = (\pi_4 \pm i\pi_5)/\sqrt{2}$, $K^0/\bar{K}^0 = (\pi_6 \pm i\pi_7)/\sqrt{2}$ and [45]

$$\begin{pmatrix} \pi^0 \\ \eta \end{pmatrix} = \begin{pmatrix} \cos\theta_{\eta\pi} & \sin\theta_{\eta\pi} \\ -\sin\theta_{\eta\pi} & \cos\theta_{\eta\pi} \end{pmatrix} \begin{pmatrix} \pi_3 \\ \pi_8 \end{pmatrix}, \quad \text{with} \quad \tan(2\theta_{\eta\pi}) = \frac{\sqrt{3}(m_u - m_d)}{(m_u + m_d - 2m_s)}. \quad (\text{B1})$$

The masses squared of the mesons are $m_{\pi^\pm}^2 = B_0(m_u + m_d)$, $m_{K^\pm}^2 = B_0(m_u + m_s)$, $m_{K^0, \bar{K}^0}^2 = B_0(m_d + m_s)$, while $m_{\pi^0}^2$ and m_η^2 are the eigenvalues of

$$\mathcal{M}_{\pi^0, \eta}^2 = \begin{pmatrix} B_0(m_u + m_d) & B_0(m_u - m_d)/\sqrt{3} \\ B_0/(m_u - m_d)/\sqrt{3} & B_0(m_u + m_d + 4m_s)/3 \end{pmatrix}. \quad (\text{B2})$$

The parameter space of interest in this work is that of resonant scattering, $m_\eta = (2 + v_R^2/4)m_{\pi^0}$ with $v_R \lesssim 0.1$ constraining the full spectrum: up to a negligible dependence on v_R , the ratios among the meson masses are fixed in term of the parameter $r_{ud} = m_u/m_d$. In particular, this implies that $m_{\pi^\pm} = (1 + \delta)m_{\pi^0}$, with δ varying from 0 to 0.075, as Fig. 3 shows.

- *Benchmark BM2.* We fix $N_f = n + 1$ with $n \geq 3$ and choose the quark mass matrix as $M = \text{diag}(m, \dots, m, \mu)$ with $0 < m < \mu$. There is a remnant $SU(n)$ symmetry under which the $N_f^2 - 1$ mesons organize as $n^2 - 1$ in the adjoint of $SU(n)$ –the pions π – as well as $2n$ in the (anti)fundamental representations –the kaons K – and one singlet corresponding to the η resonance. Their masses squared are respectively $m_\pi^2 = 2B_0m$, $m_K^2 = B_0(m + \mu)$ and $m_\eta^2 = 2B_0(m + n\mu)/(n + 1)$. The expression $m_\eta = (2 + v_R^2/4)m_\pi$ translates to $\mu = m[(n + 1)(2 + v_R^2/4)^2 - 1]/n$, which, for $v_R \lesssim 0.1$, implies $m_K^2 = B_0m(5 + 3/n) + \mathcal{O}(v_R^2)$. For $N_f = 4$ this corresponds to $\mu \simeq 5m$, $m_\eta \simeq 2m_\pi$, $m_K \simeq \sqrt{3}m_\pi$.

Cubic interactions induced by θ . The interactions in Eq. (A3) predict the decay of the η meson. The relevant structure constants are $d_{888} = -d_{338} = -1/\sqrt{3}$ in the BM1 model, while $d_{\pi_i \pi_i \eta} = \sqrt{2/n(n + 1)}$, with $i = 1, \dots, n^2 - 1$, in the BM2 model. The corresponding cubic terms are

$$\mathcal{L}_{\eta\pi\pi}^{(\text{BM1})} = \frac{B_0\theta}{\sqrt{3}f_\pi \text{Tr}M^{-1}} \cos(3\theta_{\eta\pi}) \eta \pi^0 \pi^0, \quad \mathcal{L}_{\eta\pi\pi}^{(\text{BM2})} = \frac{B_0\theta}{\sqrt{n(n + 1)}/2f_\pi \text{Tr}M^{-1}} \eta \pi \cdot \pi. \quad (\text{B3})$$

Notice that the expression for BM2 reduces to the one in BM1 if $n = 2$ and for vanishing mixing, $\theta_{\eta\pi} = 0$.

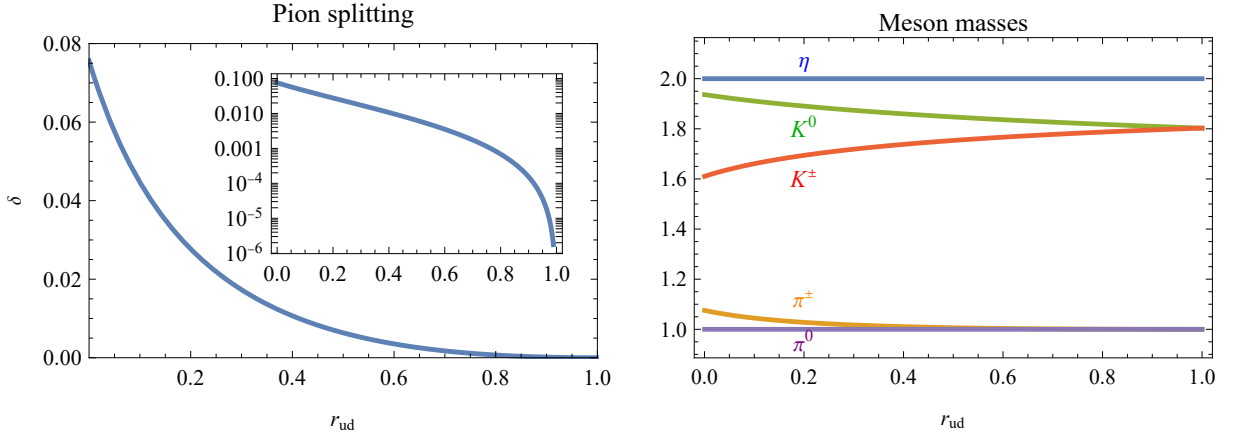


FIG. 3. *Left*: Splitting of the masses of the pions $\delta = m_{\pi^\pm}/m_{\pi^0} - 1$ as a function of r_{ud} . *Right*: Masses of the 8 mesons normalized to m_{π^0} as a function of r_{ud} . In both plots $v_R \lesssim 0.1$.

Appendix C: Boltzmann equations and Dark Matter relic density

In this section we describe the computation of the DM relic density in more detail. We focus on the parameter space for which $v_R \lesssim 0.1$. In this regime, our results are independent on the precise value of v_R . All the stable mesons contribute to the DM relic density, although their contribution depends on their mass, as in usual scenarios of co-annihilating DM, where the contribution of the heavier particles is exponentially suppressed.

Derivation of the Boltzmann equations. In general, the spectrum can be grouped in the DM particle and the other stable mesons –collectively referred to as π_{DM} – and the η resonance, which decays via θ -induced interactions. As usual, we introduce the parameter $z = m_{\text{DM}}/T$ and the yield as $Y_X = n_X/s$, where n_X is the number density and $s = 2\pi^2 g_s T^3/45$ is the total entropy density of the Universe. The Hubble rate in a radiation-dominated Universe is $H \simeq 1.66\sqrt{g_*}T^2/M_{\text{Pl}}$ (g_* being the number of relativistic d.o.f.). All the stable mesons convert to DM by means of processes that maintain chemical equilibrium among the different species. This allows us to write a Boltzmann equation for the sum of the yields of DM and its co-annihilating partners, $Y_{\pi_{\text{DM}}}$. Then, the evolution of π_{DM} and η populations is described by the following coupled Boltzmann equations:

$$\begin{cases} sH z \frac{dY_{\pi_{\text{DM}}}}{dz} = -\gamma_3(\pi_{\text{DM}}\pi_{\text{DM}}\pi_{\text{DM}} \rightarrow \pi_{\text{DM}}\pi_{\text{DM}}) \left(\frac{Y_{\pi_{\text{DM}}}^3}{Y_{\pi_{\text{DM},\text{eq}}}^3} - \frac{Y_{\pi_{\text{DM}}}^2}{Y_{\pi_{\text{DM},\text{eq}}}^2} \right) \\ \quad + 2\gamma_D(\eta \rightarrow \pi_{\text{DM}}\pi_{\text{DM}}) \left(\frac{Y_\eta}{Y_{\eta,\text{eq}}} - \frac{Y_{\pi_{\text{DM}}}^2}{Y_{\pi_{\text{DM},\text{eq}}}^2} \right) + \gamma_2(\eta\pi_{\text{DM}} \rightarrow \pi_{\text{DM}}\pi_{\text{DM}}) \left(\frac{Y_\eta}{Y_{\eta,\text{eq}}} \frac{Y_{\pi_{\text{DM}}}}{Y_{\pi_{\text{DM},\text{eq}}}} - \frac{Y_{\pi_{\text{DM}}}^2}{Y_{\pi_{\text{DM},\text{eq}}}^2} \right) \\ sH z \frac{dY_\eta}{dz} = -\gamma_D(\eta \rightarrow \pi_{\text{DM}}\pi_{\text{DM}}) \left(\frac{Y_\eta}{Y_{\eta,\text{eq}}} - \frac{Y_{\pi_{\text{DM}}}^2}{Y_{\pi_{\text{DM},\text{eq}}}^2} \right) - \gamma_2(\eta\pi_{\text{DM}} \rightarrow \pi_{\text{DM}}\pi_{\text{DM}}) \left(\frac{Y_\eta}{Y_{\eta,\text{eq}}} \frac{Y_{\pi_{\text{DM}}}}{Y_{\pi_{\text{DM},\text{eq}}}} - \frac{Y_{\pi_{\text{DM}}}^2}{Y_{\pi_{\text{DM},\text{eq}}}^2} \right), \end{cases} \quad (\text{C1})$$

where $\gamma(I)$ is the equilibrium interaction rate density for the process I , obtained by adding the individual contributions of the co-annihilating partners. For $2 \rightarrow 2$ scatterings, the latter is defined as

$$\gamma(12 \rightarrow 34) = S_{12}S_{34} \int d^3p_1 d^3p_2 f_1^{\text{eq}} f_2^{\text{eq}} \int d^3p_3 d^3p_4 (2\pi)^4 \delta^4(p_1 + p_2 - p_3 - p_4) |\mathcal{A}_{12 \rightarrow 34}|^2, \quad (\text{C2})$$

where $S_{12}(S_{34}) = 1(1/2)$ if the initial (final) particles are different (identical), f_i^{eq} is the equilibrium distribution for the particle i and \mathcal{A} is the amplitude of the process. In the non-relativistic limit, $m_{1,2} \gg T$, this reduces to $\gamma(12 \rightarrow 34) \simeq S_{12}n_{1,\text{eq}}n_{2,\text{eq}}\langle\sigma_{12 \rightarrow 34}v\rangle$, in terms of the thermal averaged cross section $\langle\sigma_{12 \rightarrow 34}v\rangle$ and the equilibrium number densities. Similar expressions hold for $n \rightarrow 2$ processes with $n \geq 1$. Detailed balance implies $\gamma_2(\pi_{\text{DM}}\pi_{\text{DM}} \rightarrow \eta\pi_{\text{DM}}) = \gamma_2(\eta\pi_{\text{DM}} \rightarrow \pi_{\text{DM}}\pi_{\text{DM}})$ and similarly for the other processes. Additional number-changing interactions, such as 4-to-2 annihilations are assumed negligible. Note that might not be the case for keV DM [11].

Furthermore, for v_R sufficiently small, 3-to-2 annihilations are dominated by the *on-shell* exchange of η (see Fig. 1 of the main text). To avoid double-counting, from the total 3-to-2 rate, one must subtract the resonant piece, associated with $\pi_{\text{DM}}\pi_{\text{DM}} \rightarrow \eta$ followed by $\eta\pi_{\text{DM}} \rightarrow \pi_{\text{DM}}\pi_{\text{DM}}$, see e.g. Ref. [52]. Here, $\gamma_3(\pi_{\text{DM}}\pi_{\text{DM}}\pi_{\text{DM}} \rightarrow \pi_{\text{DM}}\pi_{\text{DM}})$ only refers to the non-resonant piece after subtraction, which is small. In the same region of the parameter space, the inverse decay processes $\pi_{\text{DM}}\pi_{\text{DM}} \rightarrow \eta$ are strongly enhanced. As a result decays $\eta \rightarrow \pi_{\text{DM}}\pi_{\text{DM}}$ and inverse decay keep the

π_{DM} fields and η in chemical equilibrium, even after all other DM number-changing interactions have frozen-out. In terms of chemical potentials, $\mu_\eta = 2\mu_{\pi_{\text{DM}}}$ which leads to

$$\frac{Y_\eta}{Y_{\eta,\text{eq}}} = \frac{Y_{\pi_{\text{DM}}}^2}{Y_{\pi_{\text{DM},\text{eq}}}^2}. \quad (\text{C3})$$

This only works as long as the decays and inverse decays $\eta \leftrightarrow \pi_{\text{DM}}\pi_{\text{DM}}$ are both active, which places a lower bound $\theta \gtrsim \theta_{\text{min}}$, as discussed in the main text and detailed further below. We underline that the presence of the resonance is crucial, as for $m_\eta \gg m_{\text{DM}}$, the inverse decay rate gets suppressed by a factor $e^{-m_\eta/m_{\text{DM}}}$, freezing out much before than the other DM number-changing processes, invalidating Eq. (C3). All in all, the Boltzmann Eqs. (C1), under the condition Eq. (C3) simplify to

$$\begin{cases} sHz \frac{dY_{\pi_{\text{DM}}}}{dz} = - \left(\gamma_2(\eta\pi_{\text{DM}} \rightarrow \pi_{\text{DM}}\pi_{\text{DM}}) + \gamma_3(\pi_{\text{DM}}\pi_{\text{DM}}\pi_{\text{DM}} \rightarrow \pi_{\text{DM}}\pi_{\text{DM}}) \right) \left(\frac{Y_{\pi_{\text{DM}}}^3}{Y_{\pi_{\text{DM},\text{eq}}}^3} - \frac{Y_{\pi_{\text{DM}}}^2}{Y_{\pi_{\text{DM},\text{eq}}}^2} \right) \\ sHz \frac{dY_\eta}{dz} = - \gamma_2(\eta\pi_{\text{DM}} \rightarrow \pi_{\text{DM}}\pi_{\text{DM}}) \left(\frac{Y_{\pi_{\text{DM}}}^3}{Y_{\pi_{\text{DM},\text{eq}}}^2} - \frac{Y_{\pi_{\text{DM}}}^2}{Y_{\pi_{\text{DM},\text{eq}}}^2} \right) \end{cases}. \quad (\text{C4})$$

As expected, the processes $\eta\pi_{\text{DM}} \rightarrow \pi_{\text{DM}}\pi_{\text{DM}}$ change the number of DM particles as the 3-to-2 reactions do. We can then write a single Boltzmann equation for the combination $Y_{\pi_{\text{DM}}} + 2Y_\eta$,

$$sHz \frac{d(Y_{\pi_{\text{DM}}} + 2Y_\eta)}{dz} \simeq - \gamma_2(\eta\pi_{\text{DM}} \rightarrow \pi_{\text{DM}}\pi_{\text{DM}}) \left(\frac{Y_{\pi_{\text{DM}}}^3}{Y_{\pi_{\text{DM},\text{eq}}}^3} - \frac{Y_{\pi_{\text{DM}}}^2}{Y_{\pi_{\text{DM},\text{eq}}}^2} \right), \quad (\text{C5})$$

where we neglect the non-resonant piece, $\gamma_3(\pi_{\text{DM}}\pi_{\text{DM}}\pi_{\text{DM}} \rightarrow \pi_{\text{DM}}\pi_{\text{DM}})$. Furthermore, as $Y_\eta \ll Y_{\pi_{\text{DM}}}$, we can approximate $Y_{\pi_{\text{DM}}} + 2Y_\eta \simeq Y_{\pi_{\text{DM}}}$. In the non-relativistic limit, $m_{\text{DM}} \gg T$, we can write $\gamma_2 \simeq s^2 Y_{\pi_{\text{DM},\text{eq}}} Y_{\eta,\text{eq}} \langle \sigma_{\eta\pi} v \rangle$, with $\sigma_{\eta\pi} \equiv \sigma(\eta\pi_{\text{DM}} \rightarrow \pi_{\text{DM}}\pi_{\text{DM}})$, so that

$$\frac{dY_{\pi_{\text{DM}}}}{dz} \simeq - \langle \sigma_{\eta\pi} v \rangle \frac{sY_{\eta,\text{eq}}}{zH} \left(\frac{Y_{\pi_{\text{DM}}}^3}{Y_{\pi_{\text{DM},\text{eq}}}^2} - \frac{Y_{\pi_{\text{DM}}}^2}{Y_{\pi_{\text{DM},\text{eq}}}^2} \right). \quad (\text{C6})$$

The DM relic density is obtained upon numerical integration of the previous equation. As long as the condition $\theta \gtrsim \theta_{\text{min}}$ is full-filled, the DM relic density is independent of the precise value of θ . Our results are well approximated by evaluating the DM relic density as $Y_{\pi_{\text{DM},\text{eq}}}(z_{\text{fo}})$ where z_{fo} is the time at which the scatterings $\eta\pi_{\text{DM}} \rightarrow \pi_{\text{DM}}\pi_{\text{DM}}$ freeze out, estimated as $H(z_{\text{fo}}) \approx n_{\eta,\text{eq}}(z_{\text{fo}}) \langle \sigma_{\eta\pi} v \rangle$. This gives (assuming constant $g_s \simeq g_*$)

$$z_{\text{fo}} \simeq \frac{m_{\text{DM}}}{m_\eta} \log \left[\frac{\sqrt{z_{\text{fo}}}}{1.66\sqrt{g_*}} \left(\frac{m_\eta}{2\pi m_{\text{DM}}} \right)^{3/2} m_{\text{DM}} M_{\text{Pl}} \langle \sigma_{\eta\pi} v \rangle \right], \quad (\text{C7})$$

which can be solved iteratively. We find $z_{\text{fo}} \sim 15 - 25$.

Effective cross sections. The annihilation cross section $\langle \sigma_{\eta\pi} \rangle$ depends on the specific benchmark model.

- *Benchmark BM2.* The total DM relic density is the sum of the contributions of pions π and kaons K , which are maintained in chemical equilibrium through 2-to-2 scatterings, which freeze out after z_{fo} . Nonetheless, kaons are heavier and their abundance is exponentially suppressed with respect to the one of the pions as $Y_K/Y_\pi \sim \exp[-(m_K - m_{\text{DM}})z/m_{\text{DM}}]$. In the region of the parameter space that we are considering here, $m_K \simeq \sqrt{3}m_\pi$ and the exponential suppression is strong (roughly a factor $\lesssim 10^{-3}$ for $z > 10$). Kaons can thus be safely neglected and $Y_{\pi_{\text{DM}}} \simeq Y_\pi$. The only cross section relevant to determine the DM relic density is $\sigma(\eta\pi \rightarrow \pi\pi) \equiv \sigma_{\eta\pi}$. As a result, $\langle \sigma_{\eta\pi} v \rangle = \sqrt{5}m_{\text{DM}}^2(n^2 - 4)/(192\pi f_\pi^4 n^2(n + 1))$.
- *Benchmark BM1.* Here the spectrum is more involved: four kaons and π^\pm , which are stable, in addition to the lightest π^0 and the η resonance. All the stable mesons are maintained in chemical equilibrium by conversion processes such as $\pi^+\pi^- \leftrightarrow \pi^0\pi^0$ (and similar for the other species), which freeze-out after z_{fo} . While the contribution of kaons is irrelevant in analogy to the BM2 model, π^\pm cannot be neglected, as $\delta \equiv m_{\pi^\pm}/m_{\pi^0} - 1 \lesssim 0.075$. In fact, at the freeze-out of $\eta\pi_{\text{DM}} \rightarrow \pi_{\text{DM}}\pi_{\text{DM}}$, π^\pm are almost as abundant as π^0 . Therefore, $Y_{\pi_{\text{DM}}} \simeq Y_{\pi^0} + Y_{\pi^\pm} + Y_{\pi^\pm} = Y_{\pi^0} + 2Y_{\pi^\pm}$. We must take into account the $\eta\pi \rightarrow \pi\pi$ processes which involve all the 3 pions. At the leading order in the δ parameter these are given by

$$\langle \sigma(\eta\pi^0 \rightarrow \pi_{1,2}\pi_{1,2})v \rangle = \frac{529\sqrt{5}m_{\pi^0}^2}{5184\pi f_\pi^4}\delta, \quad \langle \sigma(\eta\pi_{1,2} \rightarrow \pi^0\pi_{1,2})v \rangle = \frac{49\sqrt{5}m_{\pi^0}^2}{2592\pi f_\pi^4}\delta, \quad \langle \sigma(\eta\pi^0 \rightarrow \pi^0\pi^0)v \rangle = \frac{\sqrt{5}m_{\pi^0}^2}{64\pi f_\pi^4}\delta, \quad (\text{C8})$$

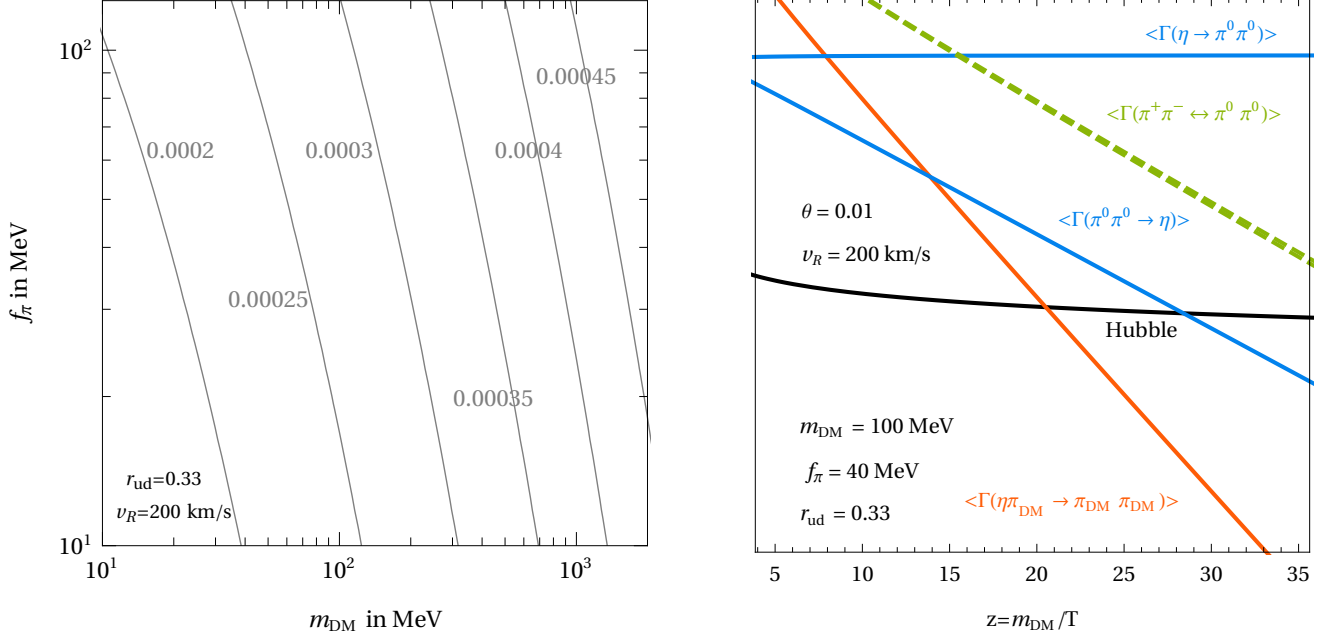


FIG. 4. *Left*: Contours of θ_{\min} as a function of m_{DM} and f_π in the BM1 model. *Right*: Thermal averaged interaction rates for the different processes compared to the Hubble rate, for values of the parameters that reproduce the DM relic abundance with $\theta > \theta_{\min}$. Notice that (inverse) decays keep η and π^0 in chemical equilibrium even for $z > z_{\text{fo}}$. Analogously $\pi^+ \pi^- \leftrightarrow \pi^0 \pi^0$ conversions keep the three pions in chemical equilibrium.

which, after accounting for combinatoric factors, are summed as

$$\langle \sigma_{\eta\pi} v \rangle \simeq \frac{1}{3} \left(\langle \sigma(\eta\pi^0 \rightarrow \pi^0\pi^0) v \rangle + 2 \langle \sigma(\eta\pi^0 \rightarrow \pi_1\pi_1) v \rangle + 2 \langle \sigma(\eta\pi_1 \rightarrow \pi^0\pi_1) v \rangle \right). \quad (\text{C9})$$

In the non-relativistic limit, this enters $\gamma(\eta\pi_{\text{DM}} \rightarrow \pi_{\text{DM}}\pi_{\text{DM}}) = n_{\eta,\text{eq}} n_{\pi_{\text{DM}},\text{eq}} \langle \sigma_{\eta\pi} v \rangle$, to be replaced in Eq. (C6).

Notice that today DM is made only by π^0 . The conversion processes $\pi^+ \pi^- \rightarrow \pi^0 \pi^0$ can efficiently deplete the π^\pm population as long as the mass splitting is $\delta \gtrsim 10^{-5}$ [26], which is realized in our setup as long as $r_{ud} \lesssim 0.95$.

Determination of θ_{\min} Eq. (C3) works as long as π_{DM} and η are kept in chemical equilibrium after the freeze-out of the reactions $\eta\pi_{\text{DM}} \rightarrow \pi_{\text{DM}}\pi_{\text{DM}}$, occurring at z_{fo} . This requires that θ is larger than a minimal value, which can be estimated as follows. We consider the thermal averaged decay and inverse decay rates

$$\langle \Gamma(\eta \rightarrow \pi_{\text{DM}}\pi_{\text{DM}}) \rangle = \frac{K_1(m_\eta/T)}{K_2(m_\eta/T)} \Gamma(\eta \rightarrow \pi_{\text{DM}}\pi_{\text{DM}}), \quad \langle \Gamma(\pi_{\text{DM}}\pi_{\text{DM}} \rightarrow \eta) \rangle = \frac{n_{\eta,\text{eq}}}{n_{\pi_{\text{DM}},\text{eq}}} \langle \Gamma(\eta \rightarrow \pi_{\text{DM}}\pi_{\text{DM}}) \rangle, \quad (\text{C10})$$

where $K_{1,2}$ are the modified Bessel functions. These processes are active as long as

$$\langle \Gamma(\eta \rightarrow \pi_{\text{DM}}\pi_{\text{DM}}) \rangle > H \quad \text{and} \quad \langle \Gamma(\pi_{\text{DM}}\pi_{\text{DM}} \rightarrow \eta) \rangle > H. \quad (\text{C11})$$

Since inverse decay rate is exponentially suppressed after $z \gtrsim 1$, to maintain the chemical equilibrium among η and π_{DM} at $z \geq z_{\text{fo}}$, it is necessary that

$$\langle \Gamma(\pi_{\text{DM}}\pi_{\text{DM}} \rightarrow \eta) \rangle \geq H \quad \text{at} \quad z = z_{\text{fo}}. \quad (\text{C12})$$

This determines the minimal value θ_{\min} as a function of $(v_R, m_{\text{DM}}, f_\pi)$. We show some reference values in Fig. 4 (left) for the BM1 model. Similar results hold the BM2 model. Notice that the dependence on v_R is not trivial: in the relevant region of the parameter space for this work, $v_R \lesssim 0.1$, we have $\Gamma(\pi_{\text{DM}}\pi_{\text{DM}} \rightarrow \eta) \propto v_R$. Hence, as v_R gets smaller, larger values of θ_{\min} are required to compensate the suppression. In Fig. 4 (right) we show the interaction rates for the different relevant processes compared with the Hubble rate for different values of the parameters in the BM1 model. Clearly, the DM production mechanism studied here works even for small values of the θ parameter, in the range of 10^{-4} .